

Design of Metal-Insulator-Metal Plasmonic Waveguide Biosensor for Disease Diagnosis

M. Sharifi^a, M. Purasl^a, and H. Tajalli^a

a Biophotonic Research Centre, Tabriz Branch Islamic Azad University, Tabriz, Iran

*Corresponding Author Email: m_sharifi66@yahoo.com

DOI: 10.71498/ijbbe.2024.1191244

ABSTRACT

Received: Nov. 22, 2024, Revised: Feb. 25, 2025, Accepted: Feb. 26, 2025, Available Online: Mar. 18, 2025

A plasmonic metal-insulator-metal (MIM) biosensor exploits the optical properties of surface plasmon resonances (SPRs) to achieve high sensitivity and specificity in biomolecule detection. The MIM structure in this study features a narrow waveguide as the insulator layer, flanked by elliptical arrays of solid metallic ovals surrounded by thin air layers. These arrays generate localized surface plasmon polaritons (LSPPs), which enhance light-matter interaction. The system operates through dual plasmonic resonances, specifically Fano resonances, resulting in a distinct transmission spectrum. Fano resonances, arising from the interference between narrow and broad resonances, produce sharp asymmetric transmission profiles that are highly sensitive to refractive index changes in surrounding biomolecules. Numerical simulations using the finite element method (FEM) confirm the sensor's ability to detect minor refractive index shifts, making it highly responsive to small biological variations. The simulation results indicate that the proposed design achieves a sensitivity of approximately 20–50 picometers for a refractive index change as small as $\Delta n=10^{-6}$. This MIM biosensor shows significant potential in applications such as point-of-care diagnostics and environmental monitoring. It can detect a wide range of biomolecules, including proteins, DNA, and pathogens, with high precision, enabling early disease detection and real-time monitoring of environmental contaminants. The enhanced sensitivity provided by Fano resonances positions this technology as a promising tool for personalized medicine, public health, and safety applications.

KEYWORDS

Biosensor, Fano Resonance, FEM, MIM waveguide.

I. INTRODUCTION

Surface plasmon polaritons (SPPs) are electromagnetic waves that propagate along the interface between a metal and a dielectric, arising from the coupling of surface plasmons within the metal and electromagnetic waves in the dielectric (1). This interaction leads to highly confined electromagnetic fields near the surface, which can be harnessed for various

applications. Extensive research on SPP-based structures has demonstrated their potential in a wide range of fields, including biosensing (2), chemical sensing (3), metamaterials (4), plasmonic nanostructures (5), and optical communication (6). Their popularity is attributed to several key advantages: the ability to miniaturize devices, rapid response times, high sensitivity to changes in the surrounding refractive index (RI), and improved light-matter interaction (7). When new sensing

materials are introduced to an SPP-based system, the effective RI shifts, causing a corresponding wavelength shift, which allows for the calculation of sensor sensitivity.

Numerous SPP-based sensors have been proposed, offering enhanced detection capabilities and reliability (8-10). Recently, Metal-Insulator-Metal (MIM) plasmonic sensors based on SPPs have gained significant attention. MIM waveguides are particularly noteworthy due to their ability to confine light at subwavelength scales, enabling nanoscale optical information transmission with high field intensities and low fabrication costs (11, 12). These properties make MIM structures ideal for applications where compact size and enhanced light interaction are crucial, such as in biosensing and optical communication.

One area of increasing interest in MIM optical biosensors is the excitation of Fano resonances (13). Fano resonances, a quantum mechanical phenomenon resulting from the interference between a discrete quantum state and a continuum of states, have unique optical properties that can be harnessed for advanced device functionalities (14). The resulting sharp asymmetric line shapes in the absorption or transmission spectra are highly sensitive to changes in the surrounding environment. Small perturbations in the medium can lead to significant shifts in the resonance position, width, and amplitude. This high sensitivity makes Fano resonances ideal for a variety of sensing applications, particularly in detecting minute changes in biological or chemical environments (15). The incorporation of Fano resonances in MIM waveguides offers exciting opportunities for the development of advanced optical devices, particularly in fields requiring precision sensing and environmental monitoring.

In this study, we propose a novel non-through Metal-Insulator-Metal (MIM) waveguide structure designed to excite Fano resonances. The configuration consists of a bus waveguide flanked by two chain resonators, each containing eight ring-shaped cavities. This arrangement enables strong light-matter

interactions and the excitation of Fano resonances within the system. To thoroughly investigate the underlying mechanisms of Fano resonance formation, we employed the finite element method (FEM) method for numerical analysis. Additionally, we explored the sensitivity of the Fano resonance to changes in the refractive index (RI) of the surrounding medium, providing insight into its potential application for high-sensitivity biosensing and environmental monitoring. The results demonstrate that the proposed MIM waveguide can be an effective platform for developing advanced optical sensors based on the detection of RI-induced shifts in Fano resonance characteristics. Several plasmonic biosensors based on surface plasmon resonance (SPR) and localized surface plasmon resonance (LSPR) have been developed in recent years, achieving sensitivities typically ranging from 100 nm/RIU to 1000 nm/RIU depending on the design and materials used (17,18) For instance, prism-based SPR sensors offer high sensitivity but often require bulky optical setups, limiting their use in point-of-care applications (19). Similarly, nanoparticle-based LSPR sensors provide nanoscale detection but may suffer from lower specificity due to broad resonance profiles (20). In contrast, the proposed MIM waveguide biosensor leverages Fano resonances to produce sharp, asymmetric transmission peaks, achieving a sensitivity on the order of tens of picometers for a refractive index change as small as $\Delta n=10^{-6}$. This represents a significant improvement in detecting subtle biomolecular changes compared to conventional SPR and LSPR sensors while maintaining a compact design suitable for integration into miniaturized diagnostic platforms.

II. DESIGN AND NUMERICAL METHOD

Figure 1 presents a two-dimensional schematic of the proposed coupling system, which comprises a Metal-Insulator-Metal (MIM) waveguide flanked by two chain resonators, each containing eight elliptical rings, all sandwiched around a central waveguide. In the figure, the blue regions represent silver (Ag), while the gray areas correspond to air, which

serves as the insulating medium. The width of the MIM waveguide is set to $w_1=70$ nm, ensuring efficient light confinement and propagation. The coupling distance between the MIM waveguide and the ring resonators is $g=10$ nm, which optimizes energy transfer between the waveguide and resonators, allowing for the excitation of Fano resonances.

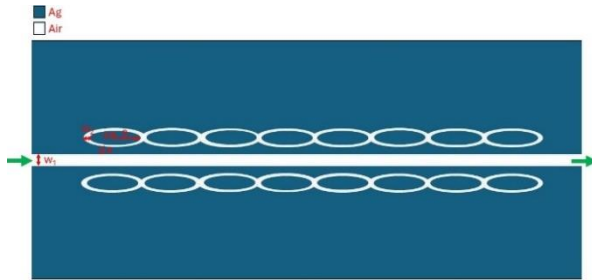


Fig. 1: Schematic of the proposed coupling system featuring a Metal-Insulator-Metal (MIM) waveguide flanked by two chains of resonators, each consisting of eight elliptical rings surrounding a central waveguide.

For the elliptical ring resonators, the air shell surrounding each ellipse has a thickness of $w_2=35$ nm, providing additional confinement of the localized surface plasmon polaritons (LSPPs). Each ellipse has a semi-major axis of $a=100$ nm and a semi-minor axis of $b=50$ nm, creating a tailored geometry that further enhances light-matter interactions. The refractive index of the medium filling the waveguide is $n=1.35$, chosen to mimic biological or chemical sensing environments. These parameters were carefully selected to maximize the sensitivity of the system to changes in the refractive index, facilitating the study of Fano resonance behavior in the proposed design.

In the computational analysis, silver (Ag) was selected as the metal material due to its favorable plasmonic properties. The relative permittivity of Ag is modeled using the Debye–Drude dispersion model, which accurately captures the frequency-dependent behavior of metals at optical frequencies. The permittivity of Ag is given by the following equation (2):

$$\varepsilon(\omega) = \varepsilon_{\infty} + \frac{\varepsilon_g - \varepsilon_{\infty}}{1 + i\omega\tau} + \frac{\sigma}{i\omega\varepsilon_0} \quad (1)$$

In Equation (1), $\varepsilon_{\infty} = 3.8344$ represents the permittivity at infinite frequency, while $\varepsilon_g = -9530.5$ is the static permittivity, indicating the low-frequency response of the metal. The term $\tau = 7.35 \times 10^{-15}$ s refers to the relaxation time, which accounts for electron scattering effects in the material, and $\sigma = 1.1486 \times 10^7$ S/m is the electrical conductivity of silver. This model provides a comprehensive description of Ag's optical properties across a broad range of frequencies. Given the MIM waveguide structure, only the fundamental transverse magnetic mode (TM_0) is supported and transmitted. As this mode is characterized by a magnetic field perpendicular to the propagation direction and the electric field confined near the metal-dielectric interface, it plays a crucial role in enabling surface plasmon polariton (SPP) excitation. Therefore, the analysis of the TM transmission mode is essential for understanding the behavior of light propagation within the MIM waveguide and optimizing the system's sensitivity to refractive index variations.

In our simulation, we numerically analyzed the spectral response of the designed MIM structure using the two-dimensional model based on FEM within the COMSOL Multiphysics platform. The lateral dimensions of the structure were set to $1.2 \times 2 \mu\text{m}$ to balance both the physical relevance of the model and computational efficiency. To achieve accurate results without excessive time costs, we focused exclusively on a 2D model. This approach allows us to capture the essential behavior of the system while optimizing the trade-off between computational accuracy and resource consumption.

To ensure precise and reliable simulations, we employed perfectly matched layer (PML) boundary conditions, which minimize reflections at the edges of the computational domain, effectively simulating an open system. A user-controlled mesh grid was implemented to optimize the balance between calculation speed and accuracy, specifically refining the mesh in areas of critical interest, such as the waveguide and resonator regions. This targeted meshing ensures that the key features of the

MIM structure are accurately resolved while maintaining computational efficiency.

The light source, generating a TM-polarized wave, was introduced at the left side of the waveguide (indicated by the green arrow) by placing an active port at the input of the simulation domain. TM polarization is essential for the excitation of surface plasmon polaritons (SPPs), which are then confined and transmitted through the MIM waveguide. To measure the transmission response, a detector was positioned at the right side of the waveguide by placing an output port. The transmission spectrum was subsequently analyzed by tracking the light propagation from the input to the output port, providing insights into the resonant behavior of the system. This setup allows us to evaluate how effectively the structure supports the excitation and transmission of SPPs and their impact on the resulting spectral properties. While the proposed MIM waveguide biosensor demonstrates promising performance in simulations, its practical implementation involves several fabrication challenges that warrant consideration. The precise construction of the elliptical ring resonators, with dimensions such as a semi-major axis of 100 nm and a semi-minor axis of 50 nm, requires advanced nanofabrication techniques, such as electron-beam lithography or focused ion beam milling, to ensure geometric accuracy. Additionally, achieving a uniform coupling distance of $g=10$ nm between the waveguide and resonators demands high precision to maintain consistent energy transfer and resonance characteristics. The integration of silver (Ag) as the plasmonic material may also pose challenges due to its susceptibility to oxidation, potentially necessitating protective coatings or alternative materials like gold (Au) in real-world applications. Addressing these fabrication hurdles through optimized processes and material selection will be critical to translating this design from a simulation to a functional device.

III. RESULTS AND DISCUSSION

As shown in Figure 2, the transmission spectrum displays two prominent asymmetrical peaks at wavelengths $\lambda=1110$ nm and $\lambda=1464$ nm, which are recognized as Fano resonances. These sharp, asymmetric peaks result from the interference between a narrow discrete resonance and a broader spectral continuum, a hallmark of Fano resonance. To explore how variations in the refractive index (RI) affect the transmission properties of the proposed MIM waveguide structure, simulations were performed by replacing the air inside the waveguide with a biomaterial medium having a refractive index of $n=1.35$. Figure 2 compares the transmission spectra for air (represented by the red solid line) and for the biomaterial (represented by the blue solid line).

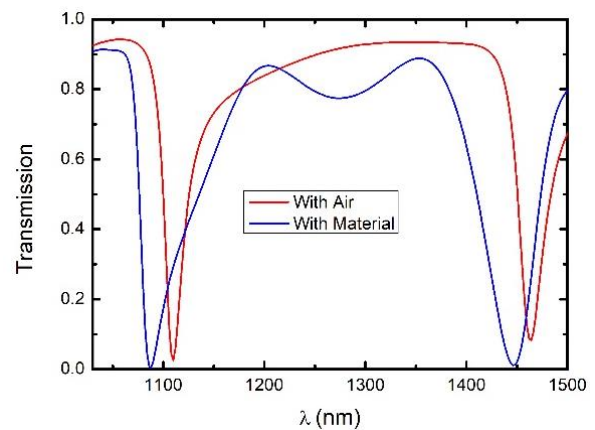


Fig. 2: Transmission spectra of the proposed MIM waveguide structure: red line for air-filled and blue line for biomaterial-filled. The shift in resonance wavelengths due to refractive index changes demonstrates the system's sensitivity and highlights the distinct Fano resonance peaks.

The results reveal a significant wavelength shift in the Fano resonance peaks as the refractive index increases from 1.0 (air) to 1.35 (biomaterial). This shift underscores the system's high sensitivity to changes in the RI, as even a small change in the refractive index leads to a substantial displacement in the transmission spectrum. The sensitivity observed is on the order of tens of picometers for a $\Delta n=10^{-6}$ change in refractive index, indicating that the MIM waveguide can detect extremely small variations in the biomaterial's RI. This exceptional sensitivity positions the

MIM waveguide system as a powerful tool for biosensing applications, where detecting subtle changes in RI—caused by the presence of biomolecules—is critical for early and precise detection. Such capabilities are crucial for developing advanced biosensors aimed at real-time, accurate monitoring of biological interactions or disease markers. To assess the biosensor's specificity for disease diagnosis, its response to biologically relevant analytes was further explored. The refractive index of $n=1.35$ used in the simulations mimics the typical RI range of biological media, such as aqueous solutions containing proteins (e.g., bovine serum albumin, $RI \approx 1.33-1.36$) or DNA strands ($RI \approx 1.34-1.37$) (21). The observed wavelength shifts in the Fano resonance peaks (e.g., from $\lambda=1110$ nm to higher wavelengths with $\Delta n=0.35$) suggest that the sensor can effectively distinguish between subtle RI variations caused by the binding of specific biomolecules. For instance, the detection of pathogens, such as viruses with RI differences on the order of 10^{-3} to 10^{-6} due to surface protein interactions, could be achieved with high precision. This specificity arises from the sharp Fano resonance profiles, which minimize overlap between adjacent resonance peaks and enhance the sensor's ability to resolve distinct biomolecular signatures. These findings indicate that the proposed MIM biosensor could be tailored for targeted detection of disease markers, such as cancer-related proteins or viral DNA, supporting its potential in personalized diagnostics.

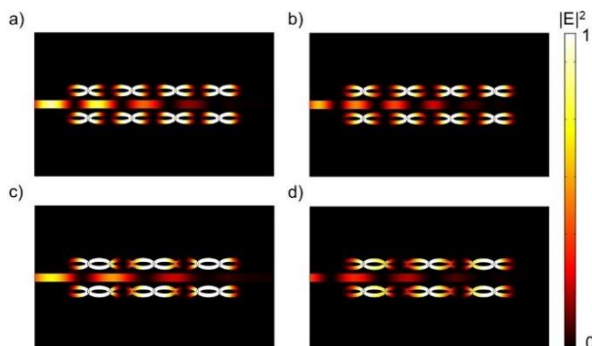


Fig. 3: Qualitative illustration of the normalized electric field intensity distribution for the first resonance at $\lambda=1110$ nm, shown for (a) air and (b) biomaterial. Similarly, the electric field distribution for the second resonance at $\lambda=1464$ nm is presented in (c) and (d), for air and biomaterial, respectively.

Figure 3 qualitatively illustrates the normalized electric field intensity distribution for each of the resonances, highlighting the critical role played by the elliptical resonators in generating Fano resonances. These elliptical resonators enhance the interaction between the localized surface plasmon polaritons (LSPPs) and the incident light, which is essential for the excitation of the Fano resonances.

In Figures 3(a) and 3(b), the field distribution for the first resonance at $\lambda=1110$ nm is shown for both air and biomaterial, respectively. The field intensity is concentrated around the elliptical resonators, demonstrating their role in confining and localizing the electromagnetic energy, which leads to the asymmetric Fano resonance profile. Similarly, Figures 3(c) and 3(d) depict the electric field distribution for the second resonance at $\lambda=1464$ nm. Here too, the elliptical resonators act as key elements in modulating the light-matter interaction. The intensity distribution in these figures reveals the wavelength-dependent behavior of the system. The shift in field localization between air and biomaterial further demonstrates the system's sensitivity to refractive index changes, with the resonance characteristics adjusting in response to the surrounding medium.

IV. CONCLUSION

In conclusion, we have demonstrated that two distinct asymmetric Fano resonances can be generated in the transmission spectra of a plasmonic system consisting of a Metal-Insulator-Metal (MIM) waveguide integrated with dual chains of elliptical ring resonators. These resonators, positioned symmetrically on either side of the waveguide, play a crucial role in inducing Fano resonances through the coherent coupling and interference between continuous (broadband) and discrete (narrowband) modes within the system. This interference results in the characteristic sharp, asymmetric spectral profiles associated with Fano resonances, which are highly sensitive to changes in the surrounding refractive index (RI). The simulation results confirm that the proposed biosensor design can achieve a sensitivity on the order of tens of picometers for

a refractive index change as small as $\Delta n=10^{-6}$. This level of sensitivity positions the sensor as a promising candidate for detecting biomolecules or other analytes in fields such as medical diagnostics, environmental monitoring, and chemical analysis. The combination of the MIM waveguide and elliptical ring resonators offers a highly effective platform for plasmonic sensing, capable of providing real-time, accurate detection of molecular interactions with excellent precision. Addressing fabrication challenges and optimizing biomolecular specificity will further enhance the practical utility of this biosensor for real-world applications. Future work will focus on experimental validation of the proposed design to confirm its simulated performance and address any unforeseen practical challenges.

REFERENCES

- [1] Zhang J, Zhang L, and Xu W. "Surface plasmon polaritons: physics and applications," *Journal of Physics D: Applied Physics*. vol.45, pp.113001, 2012.
- [2] Sharifi M, PASHAEI AH, Tajalli H, and Bahrapour A. "Design of surface plasmon resonance biosensor with one dimensional photonic crystal for detection of cancer," 2016.
- [3] Martínez J, Ródenas A, Aguiló M, Fernandez T, Solis J, and Díaz F. "Mid-infrared surface plasmon polariton chemical sensing on fiber-coupled ITO coated glass," *Optics Letters*. vol. 41, pp. 2493-2496, 2016.
- [4] Gric T and Rafailov E. "Propagation of surface plasmon polaritons at the interface of metal-free metamaterial with anisotropic semiconductor inclusions," *Optik*. vol. 254, pp.168678, 2022.
- [5] Bai Y, Li Y, Ikram M, Ren Y, Xu Y, Wang Y, et al. "Circular dichroism induced by the coupling between surface plasmon polaritons and localized surface plasmon resonances in a double-layer complementary nanostructure," *The Journal of Physical Chemistry C*. vol. 126, pp. 10159-10166, 2022.
- [6] Zhang HC, Zhang LP, He PH, Xu J, Qian C, Garcia-Vidal FJ, et al. "A plasmonic route for the integrated wireless communication of subdiffraction-limited signals," *Light: Science & Applications*. vol. 9, pp.113, 2020.
- [7] Schröder B. *Probing Light-Matter Interactions in Plasmonic Nanotips: Dissertation*, Göttingen, Georg-August Universität, 2020.
- [8] Joseph S, Sarkar S, and Joseph J. "Grating-coupled surface plasmon-polariton sensing at a flat metal-analyte interface in a hybrid-configuration. *ACS Applied Materials & Interfaces*," vol.12, pp. 46519-46529, 2020.
- [9] Kumari S, Verma YK, and Tripathi SM. "Plasmonic Ring Resonator Sensor with High Figure of Merit and Sensitivity Using Degenerate N-Doped Silicon for SPP Excitation," *Plasmonics*. pp.1-9, 2024.
- [10] Aminah NS, Lertvanithphol T, Sathukarn A, Horprathum M, Alatas H, Fauzia V, et al. Fabrication of Au coated sinusoidal grating substrates as SPP-SERS sensor chip for trace-level detection of explosive. *Optical Materials*. 2024;149:114952.
- [11] Chen H, Yan S, Cao Y, Jiang W, Yan X, Wang C, et al. "Nanoscale temperature sensors based on MIM waveguide coupling and ring-embedded nanostructures," *Frontiers in Physics*.vol.12, pp.1456177, 2024.
- [12] Lu H, Wang G, and Liu X. "Manipulation of light in MIM plasmonic waveguide systems," *Chinese Science Bulletin*. vol. 58, pp. 3607-3616, 2013.
- [13] Chen J, Li J, Liu X, Rohimah S, and Tian H, "Qi D. Fano resonance in a MIM waveguide with double symmetric rectangular stubs and its sensing characteristics," *Optics communications*.vol. 482, pp. 126563, 2021.
- [14] Sharifi M, Rezaei B, Pashaei Adl H, and Zakerhamidi MS. "Tunable Fano resonance in coupled topological one-dimensional photonic crystal heterostructure and defective photonic crystal," *Journal of Applied Physics*. Vol. 133, 2023.
- [15] Adhikari R, Chauhan D, Mola GT, and Dwivedi RP. "A review of the current state-of-the-art in Fano resonance-based plasmonic metal-insulator-metal waveguides for sensing applications," *Opto-Electronics Review*. vol. 29, 2021.
- [16] Gai H, Wang J, and Tian Q. "Modified Debye model parameters of metals applicable for broadband calculations," *Applied optics*.vol. 46, pp. 2229-2233, 2007.

- [17] Sekhwama M, Mpofu K, Sivarasu S, and Mthunzi-Kufa P. "Enhancing limit of detection in surface plasmon resonance biosensors: A sensitivity analysis for optimal performance," In *Optical Interactions with Tissue and Cells XXXV*, Vol. 12840, pp. 79-85, 2024.
- [18] Cynthia S, Ahmed R, Islam S, Ali K, and Hossain M. "Graphene based hyperbolic metamaterial for tunable mid-infrared biosensing. *RSC advances*," vol.11, pp. 7938-7945, 2021.
- [19] Puiu M and Bala C. "SPR and SPR imaging: recent trends in developing nanodevices for detection and real-time monitoring of biomolecular events," *Sensors*. vol. 16, pp. 870, 2016.
- [20] Smith NS, Abhari S, Smith LS, Altman KM, Yakkanti MR, and Malkani AL. "Results of Primary Total Knee Arthroplasty in Patients on Chronic Psychotropic Medications," *The Journal of Arthroplasty*. vol. 39, pp. S161-S166, 2024.

THIS PAGE IS INTENTIONALLY LEFT BLANK.